Complement D_{XII}

THE INFLUENCE OF THE ELECTRONIC SPIN ON THE ZEEMAN EFFECT OF THE HYDROGEN RESONANCE LINE

1. Introduction

The conclusions of complement D_{VII} relative to the Zeeman effect for the resonance line of the hydrogen atom spectrum (the $1s \longleftrightarrow 2p$ transition) must be modified to take into account the electron spin and the associated magnetic interactions. This is what we shall do in this complement, using the results obtained in chapter XII.

To simplify the discussion, we shall neglect effects related to nuclear spin (which are much smaller than those related to the electron spin). Therefore, we shall not take the hyperfine coupling W_{hf} (chap. XII, § B-2) into account, choosing the Hamiltonian H in the form :

$$H = H_0 + W_f + W_Z \tag{1}$$

H_0 is the electrostatic Hamiltonian studied in chapter VII (§ C), W_f, the sum of the fine structure terms (chap. XII, §B-1):

$$W_f = W_{mv} + W_D + W_{SO} \tag{2}$$

and W_Z, the Zeeman Hamiltonian (chap. XII, §E-1) describing the interaction of the atom with a magnetic field $\mathbf{B}_0$ parallel to Oz:

$$W_Z = \omega_0(L_z + 2S_z) \tag{3}$$

where the Larmor angular frequency ω_0 is given by:

$$\omega_0 = -\frac{q}{2m_e} B_0 \tag{4}$$

[we shall neglect ω_n relative to ω_0; see formula (E-4) of chapter XII].

We shall determine the eigenvalues and eigenvectors of H by using a method analogous to that of §E of chapter XII : we shall treat W_f and W_Z like perturbations of H_0. Although they have the same unperturbed energy, the $2s$ and $2p$ levels can be studied separately since they are connected neither by W_f (chap. XII, §C-2-a-β) nor by W_Z. In this complement, the magnetic field $\mathbf{B}_0$ will be called weak or strong, depending on whether W_Z is small or large compared to W_f. Note that the magnetic fields considered here to be "weak" are those for which W_Z is small compared to W_f but large compared to W_{hf}, which we have neglected. These "weak fields" are therefore much stronger than those treated in § E of chapter XII.

Once the eigenstates and eigenvalues of H have been obtained, it is possible to study the evolution of the mean values of the three components of the electric dipole moment of the atom. Since an analogous calculation was performed in detail in complement $\mathrm{D_{VII}}$, we shall not repeat it. We shall merely indicate, for weak fields and for strong fields, the frequencies and polarization states of the various Zeeman components of the resonance line of hydrogen (the Lyman α line).

2. The Zeeman diagrams of the 1*s* and 2*s* levels

We saw in § D-1-b of chapter XII that W_f shifts the $1s$ level as a whole and gives rise to only one fine-structure level, $1s_{1/2}$. The same is true for the $2s$ level, which becomes $2s_{1/2}$. In each of these two levels, we can choose a basis:

$$\left\{ \left| n; l = 0; m_L = 0; m_S = \pm \frac{1}{2}; m_I = \pm \frac{1}{2} \right\rangle \right\} \tag{5}$$

of eigenvectors common to H_0, $\mathbf{L}^2$, L_z, S_z, I_z (the notation is identical to that of chapter XII; since H does not act on the proton spin, we shall ignore m_I in all that follows).

The vectors (5) are obviously eigenvectors of W_Z with eigenvalues $2m_S\hbar\omega_0$. Thus, each $1s_{1/2}$ or $2s_{1/2}$ level splits, in a field B_0, into two Zeeman sublevels of energies:

$$E(n; l = 0; m_L = 0; m_S) = E(ns_{1/2}) + 2m_S\hbar\omega_0 \tag{6}$$

where $E(ns_{1/2})$ is the zero-field energy of the $ns_{1/2}$ level, calculated in §§ C-2-b and D-1-b of chapter XII. The Zeeman diagram of the $1s_{1/2}$ level (as well as the one for the $2s_{1/2}$ level) is therefore composed of two straight lines of slopes $+1$ and -1 (fig. 1), corresponding, respectively, to the two possible orientations of the spin relative to $\mathbf{B}_0$ ($m_S = +1/2$ and $m_S = -1/2$).

Comparison of figure 1 and figure 9 of chapter XII shows that to neglect, as we are doing here, the effects related to nuclear spin amounts to considering fields $\mathbf{B}_0$ which are so large that $W_Z \gg W_{hf}$. We are then in the asymptotic region of the diagram of figure 9 of chapter XII, where we can ignore the splitting of the energy levels due to the proton spin and hyperfine coupling.

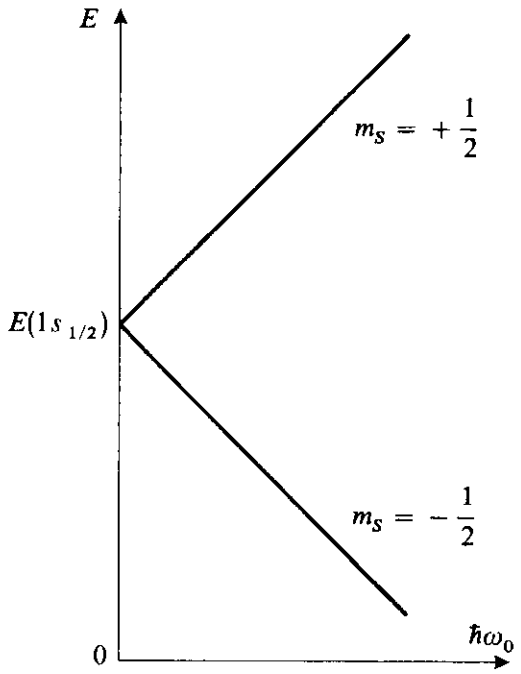

FIGURE 1

The Zeeman diagram of the $1s_{1/2}$ level when the hyperfine coupling W_{hf} is neglected. The ordinate of the point at which the two levels $m_S = \pm 1/2$ cross is the energy of the $1s_{1/2}$ level (i.e, the eigenvalue $-E_1$ of H_0, corrected for the global shift produced by the fine-structure Hamiltonian W_f). Figure 9 of chapter XII gives an idea of the modifications of this diagram produced by W_{hf}.

3. The Zeeman diagram of the 2*p* level

In the six-dimensional $2p$ subspace, we can choose one of the two bases:

$$\{ \mid n = 2; l = 1; m_L; m_S \rangle \} \tag{7}$$

or:

$$\{ \mid n = 2; l = 1; J; m_J \rangle \} \tag{8}$$

adapted, respectively, to the individual angular momenta $\mathbf{L}$ and $\mathbf{S}$ and to the total angular momentum $\mathbf{J} = \mathbf{L} + \mathbf{S}$ [*cf.* (36-a) and (36-b) of complement A_X].

The terms W_{mv} and W_D which appear in expression (2) for W_f shift the $2p$ level as a whole. Therefore, to study the Zeeman diagram of the $2p$ level, we simply diagonalize the 6×6 matrix which represents $W_{SO} + W_Z$ in either one of the two bases, (7) or (8). Actually, since W_Z and $W_{SO} = \xi_{2p}\mathbf{L} \cdot \mathbf{S}$ both commute with $J_z = L_z + S_z$, this 6×6 matrix can be broken down into as many submatrices as there are distinct values of m_J. Thus, there appear two one-dimensional submatrices (corresponding respectively to $m_J = +3/2$ and $m_J = -3/2$) and two two-dimensional submatrices (corresponding respectively to $m_J = +1/2$ and $m_J = -1/2$). The calculation of the eigenvalues and associated eigenvectors (which is very much like that of § E-4 of chapter XII) presents no difficulties and leads to the Zeeman diagram shown in figure 2. This diagram is composed of two straight lines and four hyperbolic branches.

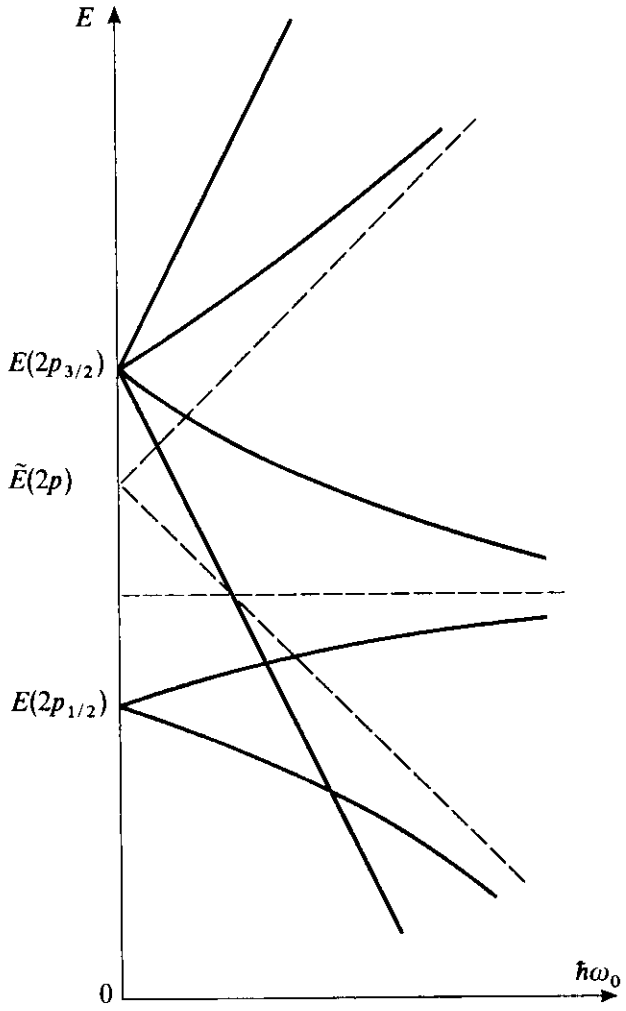

FIGURE 2

The Zeeman diagram of the $2p$ level when the hyperfine coupling W_{hf} is neglected. In a zero field, we find the fine-structure levels, $2p_{1/2}$ and $2p_{3/2}$. The Zeeman diagram is composed of two straight lines and two hyperbolas (for which the asymptotes are shown in dashed lines). The hyperfine coupling W_{hf} would significantly modify this diagram only in the neighborhood of $\omega_0 = 0$. $\tilde{E}(2p)$ is the $2p$ level energy (the eigenvalue $-E_I/4$ of H_0) corrected for the global shift produced by $W_{mv} + W_D$

In a zero field, the energies depend only on J. We obtain the two fine-structure levels, $2p_{3/2}$ and $2p_{1/2}$, already studied in § C of chapter XII, whose energies are equal to:

$$E(2p_{3/2}) = \tilde{E}(2p) + \frac{1}{2}\xi_{2p}\hbar^2 \tag{9}$$

$$E(2p_{1/2}) = \tilde{E}(2p) - \xi_{2p}\hbar^2 \tag{10}$$

$\tilde{E}(2p)$ is the $2p$ level energy $E(2p)$ corrected for the global shift due to W_{mv} and W_D [*cf.* expressions (C-8) and (C-9) of chapter XII]. ξ_{2p} is the constant which appears in the restriction $\xi_{2p}\mathbf{L} \cdot \mathbf{S}$ of W_{SO} to the $2p$ level [*cf.* expression (C-13) of chapter XII].

In weak fields ($W_Z \ll W_{SO}$), the slope of the energy levels can also be obtained by treating W_Z like a perturbation of W_f. It is then necessary to diagonalize the 4×4 and 2×2 matrices representing W_Z in the $2p_{3/2}$ and $2p_{1/2}$ levels. Calculations analogous to those of § E-2 of chapter XII show that these two submatrices are respectively proportional to those which represent $\omega_0 J_z$ in the same subspaces.

The proportionality coefficients, called "Landé factors" (*cf.* complement D_X, §3), are equal, respectively, to*:

$$g(2p_{3/2}) = \frac{4}{3} \tag{11}$$

$$g(2p_{1/2}) = \frac{2}{3} \tag{12}$$

In weak fields, each fine-structure level therefore splits into $2J + 1$ equidistant Zeeman sublevels. The eigenstates are the states of the "coupled" basis, (8), corresponding to the eigenvalues:

$$E(J, m_J) = E(2p_J) + m_J\, g(2p_J)\, \hbar\omega_0 \tag{13}$$

where the $E(2p_J)$ are given by expressions (9) and (10).

In strong fields ($W_Z \gg W_{SO}$), we can, on the other hand, treat $W_{SO} = \xi_{2p}\mathbf{L} \cdot \mathbf{S}$ like a perturbation of W_Z, which is diagonal in basis (7). As in § E-3-b of chapter XII, it can easily be shown that only the diagonal elements of $\xi_{2p}\mathbf{L} \cdot \mathbf{S}$ are involved when the corrections are calculated to first order in W_{SO}. Thus, we find that in strong fields, the eigenstates are the states of the "decoupled" basis, (7), and the corresponding eigenvalues are:

$$E(m_L, m_S) = \tilde{E}(2p) + (m_L + 2m_S)\hbar\omega_0 + m_L m_S\, \hbar^2 \xi_{2p} \tag{14}$$

Formula (14) gives the asymptotes of the diagram of figure 2.

As the magnetic field B_0 increases, we pass continuously from basis (8) to basis (7). The magnetic field gradually decouples the orbital angular momentum and the spin. This situation is the analogue of the one studied in §E of chapter XII, in which the angular momenta **S** and **I** were coupled or decoupled, depending on the relative importance of the hyperfine and Zeeman terms.

4. The Zeeman effect of the resonance line

a. STATEMENT OF THE PROBLEM

Arguments of the same type as those of §2-c of complement D_{VII} (see, in particular, the comment at the end of that complement) show that the optical transition between a $2p$ Zeeman sublevel and a $1s$ Zeeman sublevel is possible only if the matrix element of the electric dipole operator $q\mathbf{R}$ between these two states is different from zero**. In addition, depending on whether it is the $q(X + iY)$, $q(X - iY)$ or qZ operator which has a non-zero matrix element between the two

* These Landé factors can be calculated directly from formula (43) of complement D_X.

** The electric dipole, since it is an odd operator, has no matrix elements between the $1s$ and $2s$ states, which are both even. This is why we are ignoring the $2s$ states here.

Zeeman sublevels under consideration, the polarization state of the emitted light is σ^+, σ^- or π. Therefore, we use the previously determined eigenvectors and eigenvalues of H in order to obtain the frequencies of the various Zeeman components of the hydrogen resonance line and their polarization states.

COMMENT:

The $q(X + iY)$, $q(X - iY)$ and qZ operators act only on the orbital part of the wave function and cause m_L to vary, respectively, by $+1$, -1 and 0 (*cf.* complement D_{VII}, § 2-c); m_S is not affected. Since $m_J = m_L + m_S$ is a good quantum number (whatever the strength of the field B_0), $\Delta m_J = +1$ transitions have a σ^+ polarization; $\Delta m_J = -1$ transitions, a σ^- polarization; and $\Delta m_J = 0$ transitions, a π polarization.

b. THE WEAK-FIELD ZEEMAN COMPONENTS

Figure 3 shows the weak-field positions of the various Zeeman sublevels resulting from the $1s_{1/2}$, $2p_{1/2}$ and $2p_{3/2}$ levels, obtained from expressions (6), (13), (11) and (12). The vertical arrows indicate the various Zeeman components of the resonance line. The polarization is σ^+, σ^- or π, depending on whether $\Delta m_J = +1$, -1 or 0.

Figure 4 shows the positions of these various components on a frequency scale, relative to the zero-field positions of the lines. The result differs notably from that of complement D_{VII} (see figure 2 of that complement), where, observing in a direction perpendicular to $\mathbf{B}_0$, we had three equidistant components of polarization σ^+, π, σ^-, separated by a frequency difference $\omega_0/2\pi$.

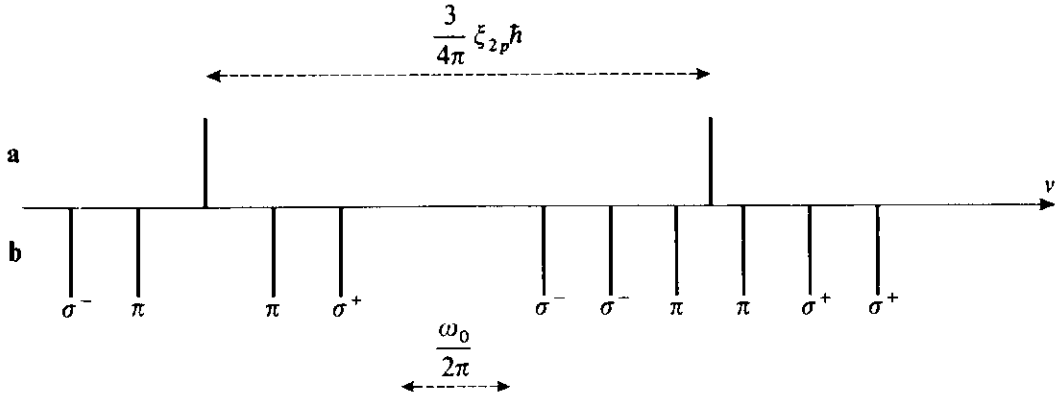

FIGURE 4

Frequencies of the various Zeeman components of the hydrogen resonance line.
a) In a zero field: two lines are observed, separated by the fine-structure splitting $3\xi_{2p}\hbar/4\pi$ (ξ_{2p} is the spin-orbit coupling constant of the $2p$ level) and corresponding respectively to the transitions $2p_{3/2} \longleftrightarrow 1s_{1/2}$ (the line on the right-hand side of the figure) and $2p_{1/2} \longleftrightarrow 1s_{1/2}$ (the line on the left-hand side).
b) In a weak field B_0: each line splits into a series of Zeeman components whose polarizations are indicated; $\omega_0/2\pi$ is the Larmor frequency in the field B_0.

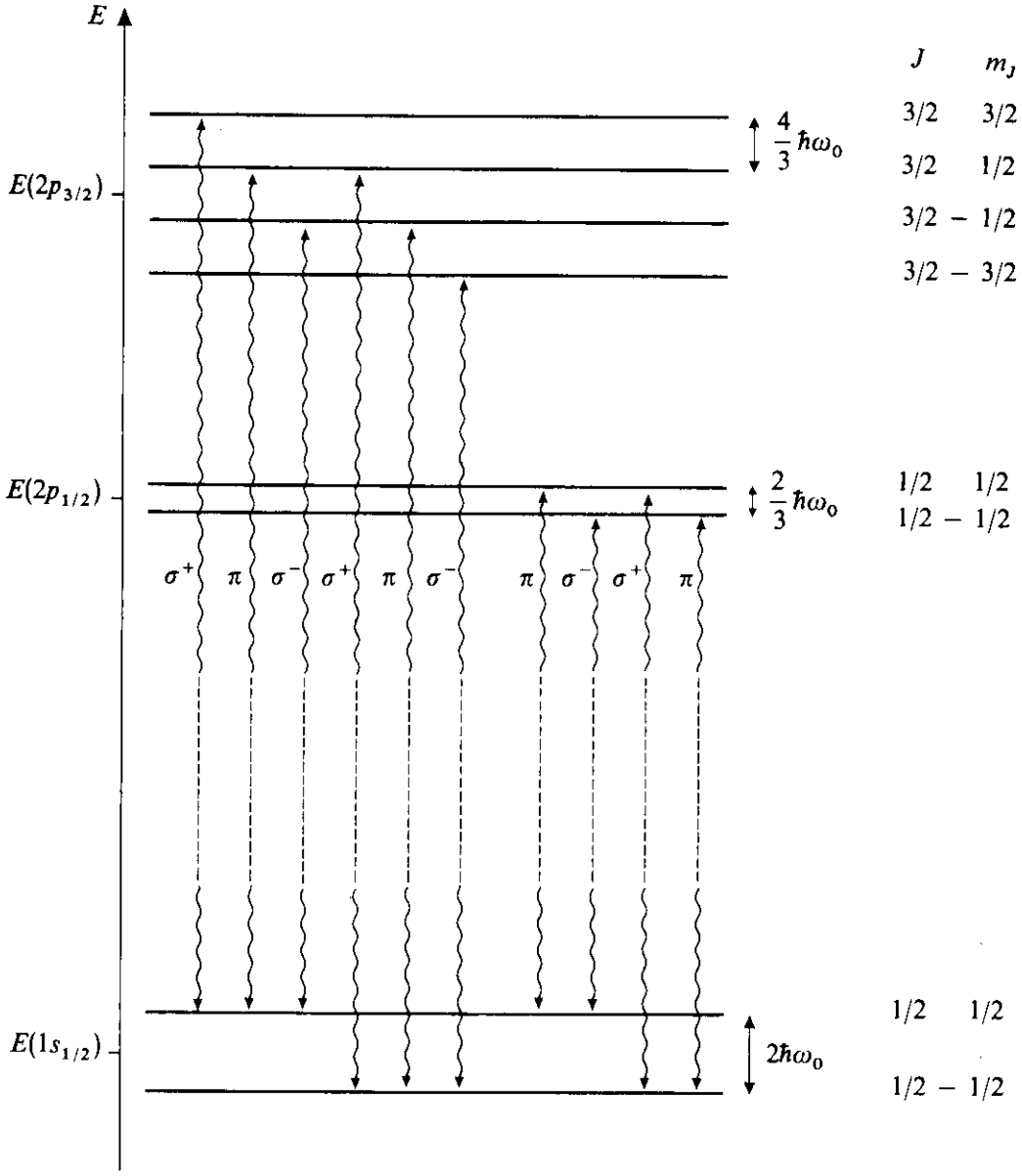

FIGURE 3

The disposition, in a weak field, of the Zeeman sublevels arising from the fine-structure levels, $1s_{1/2}$, $2p_{1/2}$, $2p_{3/2}$ (whose zero-field energies are marked on the vertical energy scale). On the right-hand side of the figure are indicated the splittings between adjacent Zeeman sublevels (for greater clarity, these splittings have been exaggerated with respect to the fine-structure splitting which separates the $2p_{1/2}$ and $2p_{3/2}$ levels), as well as the values of the quantum numbers J and m_J associated with each sublevel. The arrows indicate the Zeeman components of the resonance line, each of which has a well-defined polarization, σ^+, σ^- or π.

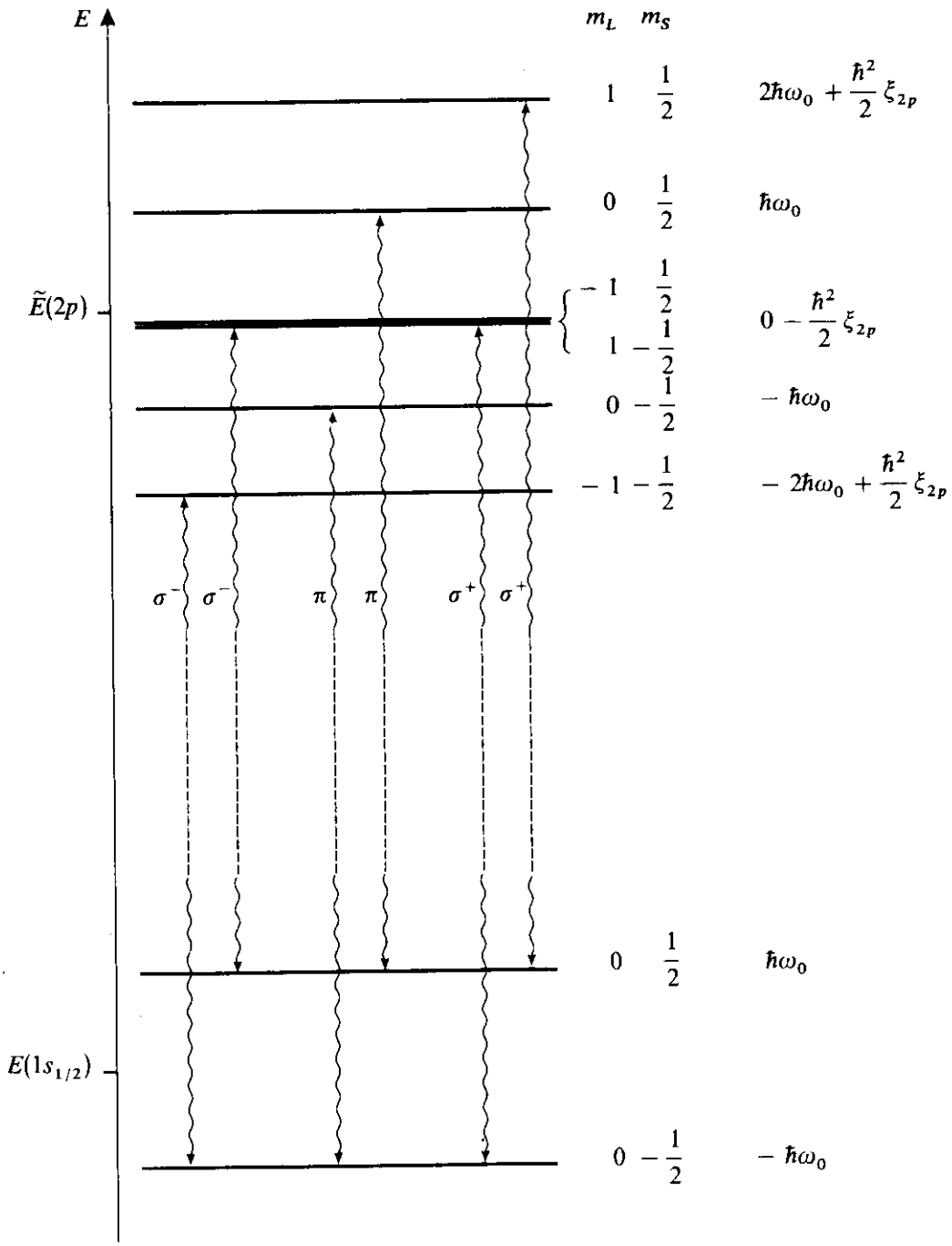

FIGURE 5

The disposition, in a strong field (decoupled fine structure), of the Zeeman sublevels arising from the $1s$ and $2p$ levels. On the right-hand side of the figure are indicated the values of the quantum numbers m_L and m_S associated with each Zeeman sublevel, as well as the corresponding energy, given relative to $E(1s_{1/2})$ or $\tilde{E}(2p)$. The vertical arrows indicate the Zeeman components of the resonance line.

c. THE STRONG-FIELD ZEEMAN COMPONENTS. THE PASCHEN-BACK EFFECT

Figure 5 shows the strong-field positions of the Zeeman sublevels arising from the $1s$ and $2p$ levels [see expressions (6) and (14)]. To first order in W_{SO}, the degeneracy between the states $|m_L = -1, m_S = 1/2\rangle$ and $|m_L = 1, m_S = -1/2\rangle$ is not removed. The vertical arrows indicate the Zeeman components of the resonance line. The polarization is σ^+, σ^- or π, depending on whether $\Delta m_L = +1$, -1 or 0 (recall that in an electric dipole transition, the quantum number m_S is not affected).

The corresponding optical spectrum is shown in figure 6. The two π transitions have the same frequency (*cf.* fig. 5). On the other hand, there is a small splitting, $\hbar\xi_{2p}/2\pi$, between the frequencies of the two σ^+ transitions and between those of the two σ^- transitions. The mean distance between the σ^+ doublet and the π line (or between the π line and the σ^- doublet) is equal to $\omega_0/2\pi$. The spectrum of figure 6 is therefore similar to that of figure 2 of complement D_{VII}. Furthermore,

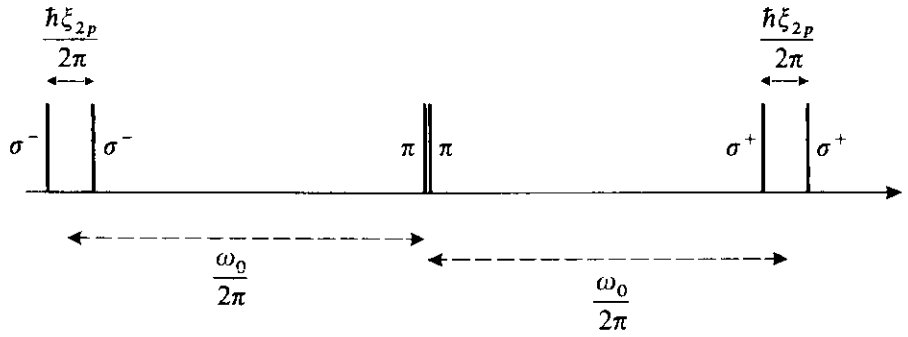

FIGURE 6

The strong-field positions of the Zeeman components of the hydrogen resonance line. Aside from the splitting of the σ^+ and σ^- lines, this spectrum is identical to the one obtained in complement D_{VII}, where the effects related to electron spin were ignored.

the splitting of the σ^+ and σ^- lines, due to the existence of the electron spin, is easy to understand. In strong fields, **L** and **S** are decoupled. Since the $1s \longleftrightarrow 2p$ transition is an electric dipole transition, only the orbital angular momentum **L** of the electron is affected by the optical transition. An argument analogous to the one in §E-3-b of chapter XII shows that the magnetic interactions related to the spin can be described by an "internal field" which adds to the external field $\mathbf{B}_0$ and whose sign changes, depending on whether the spin points up or down. It is this internal field that causes the splitting of the σ^+ and σ^- lines (the π line is not affected, since its quantum number m_L is zero).

References and suggestions for further reading:

Cagnac and Pebay-Peyroula (11.2), chaps. XI and XVII (especially §5-A of that chapter); White (11.5), chap. X; Kuhn (11.1), chap. III, §F; Sobel'man (11.12), chap. 8, § 29.